Transient Thermal Analysis of Solidification in a Centrifugal Casting for Composite Materials Containing Particle Segregation

C.G. KANG and P.K. ROHATGI

One-dimensional heat-transfer analysis during centrifugal casting of aluminum alloy and copper base metal matrix composites containing Al_2O_3, SiC_p, and graphite particles has been studied. The model of the particle segregation is calculated by varying the volume fraction during centrifugal casting, and a finite difference technique has been adopted. The results indicate that the thickness of the region in which dispersed particles are segregated due to the centrifugal force is strongly influenced by the speed of rotation of the mold, the solidification time, and the density difference between the base alloy and the reinforcement. In the case where the base alloy density is larger than that of the particles, the thickness of the particle-rich region near the inner periphery decreases with an increase in speed, thereby increasing the volume fraction of dispersion. The solidification time of the casting is also dependent upon the speed of rotation of the mold, and it decreases with an increase in speed. This study also indicates that the presence of particles increases the solidification time of the casting.

I. INTRODUCTION

DURING centrifugal casting processing of metal matrix composites,[1-4] segregation of particles occurs due to centrifugal forces, either to the outer or to the inner part of the casting, depending on the relative densities of particles and the matrix. Various processing parameters, such as pouring temperature, solidification time, pouring pattern, and thermal properties of the particles and matrix, will significantly influence the spatial arrangement of dispersed particles and the solidification microstructure which evolve during the centrifugal casting of composites.

Determination of temperature distribution during the centrifugal casting process and further determination of the solidification time of centrifugal castings by experimental techniques are very difficult, as the mold rotates at a very high speed during solidification. Because of this, accurate data on solidification time of centrifugal casting are not available. In particular, no data are available on the solidification time during centrifugal casting of metal matrix composites. Therefore, it is necessary to estimate the solidification time and the influence of other processing parameters on the solidification time in the case of centrifugal casting of metal matrix composites through indirect means. Analytical methods involving heat- and mass-transfer analysis can be useful under such circumstances.

Estimation of the solidification time and temperature distribution during solidification through heat- and mass-transfer analysis under realistic conditions in an alloy containing dispersed particles or fiber is a complex problem. The situation is further complicated in the case of centrifugal castings as the moving particles disturb the temperature equilibrium. Also, the segregation of particles either at the inner periphery or at the outer periphery significantly influences the heat-transfer coefficient at the metal-mold interface and the thermophysical properties of the solidifying material.

The existing heat-transfer models used by various investigators[5,6,7] predict temperature distribution in the mold and the molten metal for monolithic alloys for very simple cases. In recent years, one-dimensional analysis of heat flow in the presence of one or a greater number of particles has been completed.[8] However, such analyses are not applicable to a solidifying slurry when it is centrifuged.

In the process of centrifugal casting, the reported modeling[19] is limited for phase transformation considering the latent heat of solidification. The temperature distribution of the alloy can have an effect on a particle's moving velocity. However, it was assumed as negligible in the reported modeling. The present study describes results of a heat-transfer analysis of centrifugal casting of metal matrix composites by one-dimensional analysis considering the thermal mechanical properties due to particles moving as a function of temperature. These theoretical predictions were compared with Lajoye and Suery's results.[19] As a first step, the positions of the dispersed particles at a given time have been analyzed. Second, temperature distributions in the mold and the solidifying metal have been analyzed at different time intervals. Last, using these temperature distributions, solidification times for different centrifugal speeds, initial mold temperature, and pouring temperature of molten metal have been estimated.

II. ANALYSIS

A. *Heat Conduction Model*

A schematic model representation of the system of centrifugal casting of a metal matrix composites cylinder is shown in Figure 1. The heat is conducted away from the liquid at temperature T_{lc} through a graphite mold at temperature T_g. Heat is also radiated away at the inner surface

C.G. KANG, Associate Professor, is with the Department of Mechanical and Precision Engineering, Engineering Research Center for Net Shape and Die Manufacturing, Pusan National University, Pusan 609-735, Korea. P.K. ROHATGI, Professor, is with the Materials Department, University of Wisconsin–Milwaukee, Milwaukee, WI 53211.

Manuscript submitted August 26, 1994.

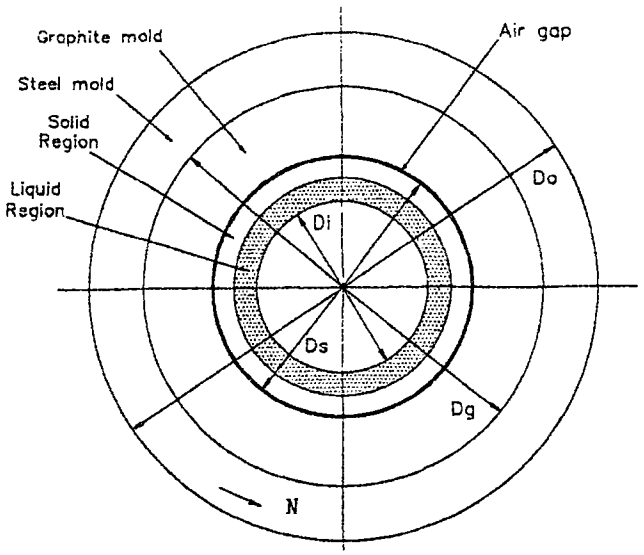

Fig. 1—Schematic representation of the complete system of centrifugal aluminum composites with particle segregation and solidification interface.

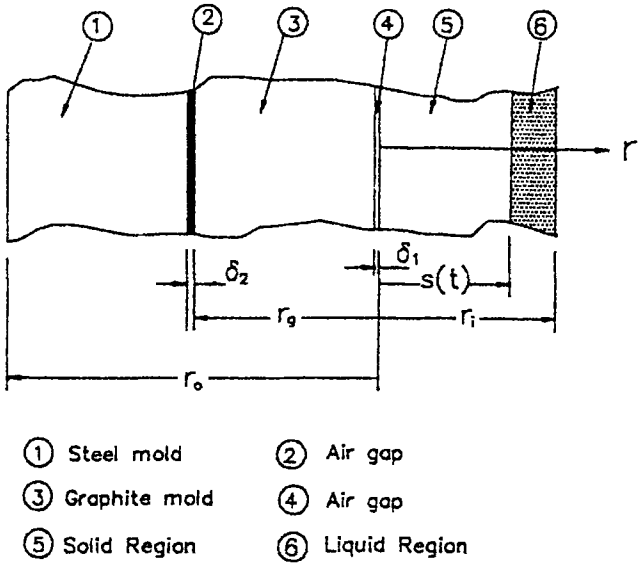

Fig. 2—One-dimensional model to calculate the temperature distribution and solidification interface.

of the cylinder being cast. The dispersed particles are within the liquid at temperature T_{lc}. As the liquid slurry solidifies by conduction heat transfer through the graphite mold, the solidification front moves away from the graphite mold toward the center of rotation. Natural convection and movement of the particles due to buoyancy have not been considered in the present study, even though it is recognized that they may have some bearing on heat transfer. The solidification fronts can be divided into planar, cellular, and dendritic morphology.[9] The interface position between the solid and liquid regions is calculated by assuming the interface to be planar. In addition, it is assumed that there is no interface thermal resistance between the particles and the liquid metal. A numerical model and the coordinate system of the centrifugally cast aluminum composite materials cylinder are shown in Figure 2 for $\rho_l > \rho_p$.

We define the coordinate system with the origin at the outside casting surface, $r = 0$, outside surface of steel mold, $r = -r_0$, and outside surface of graphite mold $r = -r_g$. The thickness of the solidified front at a given time is represented by $s(t)$. The problem then is to find the time taken for the front to move from $r = 0$ to $r = r_i$, the inside casting boundary or the inner surface of the cylinder.

The heat transfer due to conduction in the steel mold can be written in cylindrical coordinates as

$$\frac{\partial T_m}{\partial t} = \alpha_m \left(\frac{\partial^2 T_m}{\partial r^2} + \frac{1}{r} \frac{\partial T_m}{\partial r} \right) \qquad [1]$$

The heat transfer due to conduction in the graphite mold is given by

$$\frac{\partial T_g}{\partial t} = \alpha_g \left(\frac{\partial^2 T_g}{\partial r^2} + \frac{1}{r} \frac{\partial T_g}{\partial r} \right) \qquad [2]$$

Further, heat transfer due to conduction in the solidified region of the composite, which is near the graphite mold, is given by

$$\frac{\partial T_{sc}}{\partial t} = \alpha_{sc} \left(\frac{\partial^2 T_{sc}}{\partial r^2} + \frac{1}{r} \frac{\partial T_{sc}}{\partial r} \right) \qquad [3]$$

Heat conduction in the region of the composite which is still liquid is given by

$$\frac{\partial T_{lc}}{\partial t} = \alpha_{lc} \left(\frac{\partial^2 T_{lc}}{\partial r^2} + \frac{1}{r} \frac{\partial T_{lc}}{\partial r} \right) \qquad [4]$$

where

$$\alpha_g = \frac{k_g}{\rho_g C_g} \quad \alpha_m = \frac{k_m}{\rho_m C_m}$$
$$\alpha_{lc} = \frac{k_{lc}}{\rho_{lc} C_{lc}} \quad \alpha_{sc} = \frac{k_{sc}}{\rho_{sc} C_{sc}} \qquad [5]$$

The α_{lc} and α_{sc} have been determined by the volume fraction of particles due to particles moving owing to the density difference between the liquid melt and particles.

The thermal conductivity of the composite in either the liquid or solid region is determined by the rule of mixtures described as follows as a function of volume fraction $V_f(t)$ with various time t.

$$k_{sc} = [1 - V_f(t)]k_s + V_f(t)k_p$$
$$k_{lc} = [1 - V_f(t)]k_l + V_f(t)k_l \qquad [6]$$

where the volume fraction, $V_f(t)$, depends on the viscosity of the alloy, particle size, mold rotation speed, and difference in density between particle and alloy.

In a similar manner, the density and specific heat of composites as estimated by the rule of mixtures are described as follows:

$$\rho_{lc} = [1 - V_f(t)]\rho_L + V_f\rho_p$$
$$\rho_{sc} = [1 - V_f(t)]\rho_s + V_f\rho_p$$
$$C_{sc} = [1 - V_f(t)]C_s + V_fC_p$$
$$C_{lc} = [1 - V_f(t)]C_L + V_fC_p \qquad [7]$$

The thermal conductivity and specific heat of the com-

posite in either the liquid or solid region are calculated by the rule of mixtures.

Convection heat transfer occurs at the inner surface of the cylinder $r = r_i$. The controlling equation can be written as

$$q_i = h_2(T_{ri} - T_{mi}) \quad [8]$$

However, the rate of solidification of the liquid composite slurry inside the mold is significantly controlled by the air gap formation at the solid region–graphite mold interface, $r = \delta_1$, and also to some extent by the presence of air at the interface δ_2 between the graphite mold and the steel mold. These are taken into account in the heat-transfer equation while calculating temperature profiles. Therefore, the boundary conditions by the absence of air gap at the interface between the graphite mold and the steel mold are as follows:

$$r = 0,\ k_{sc}\frac{\partial T_{sc}}{\partial r} = h_1\,(T_{oc} - T_{gi}) \quad [9]$$

$$r = -\delta_1,\ -k_g\frac{\partial T_g}{\partial r} = h_1\,(T_{oc} - T_{gi}) \quad [10]$$

$$\delta = -r_g,\ -k_g\frac{\partial T_g}{\partial r} = h_4\,(T_{go} - T_{mi}) \quad [11]$$

$$\delta = -(r_g + \delta_2),\ -k_m\frac{\partial T_m}{\partial r} = h_4\,(T_{go} - T_{mi}) \quad [12]$$

$$\delta = -r_0,\ k_m\frac{\partial T_g}{\partial r} = h_3\,(T_m - T_{oa}) \quad [13]$$

$$r = s(t),\ T_{sc} = T_{lc} = T_f \quad [14]$$

$$r = s(t),\ k_{sc}\frac{\partial T_{sc}}{\partial r} - k_{lc}\frac{\partial T_{lc}}{\partial r} = H\rho_{sc}\frac{\partial s(t)}{\partial t} \quad [15]$$

By considering in sequence all the preceding heat-transfer equations and by solving them numerically, it is possible to establish the temperature distribution in the graphite mold and the solidifying liquid metal slurry. For solving these equations, a finite difference technique was adopted and a moving boundary problem was considered. The moving boundary was fixed by standard coordinate transformation.[10,11] Consider Eqs. [3] and [4], in solid and liquid regions, $0 < r < s(t)$ and $s(t) < r < r_i$, respectively.

Then the moving boundary between the solid and liquid can be fixed by the coordinate transformation:

$$\text{solid region of composites: } \xi = \frac{r}{s(t)} \qquad (0 \le r \le s(t)) \quad [16]$$

$$\text{liquid region of composites: } \eta = \frac{r - s(t)}{r_i - s(t)} \quad (s(t) \le r \le n) \quad [17]$$

so that $0 \le \xi \le 1$ and $0 \le \eta \le 1$ in each region, respectively. By using Eq. [16], the transformed governing for Eq. [3] and the boundary conditions to the solid region, Eqs. [9] and [14], are written as follows, respectively:

$$\frac{\partial T_{sc}}{\partial t} = \alpha_{sc}\left[\xi\frac{1}{s(t)}\frac{\partial s(t)}{\partial t} + \frac{1}{r}\frac{1}{s(t)}\right]\frac{\partial t_{sc}}{\partial \xi} + \alpha_{sc}\frac{1}{s^2(t)}\frac{\partial^2 T_{sc}}{\partial \xi^2} \quad (0 \le \xi \le 1) \quad [18]$$

$$\xi = 0,\ k_{sc}\frac{\partial T_{sc}}{\partial \xi}\frac{\partial \xi}{\partial r} = h_1(T_{oc} - T_{gi}) \quad [19]$$

$$\xi = 1,\ T_{sc} = T_{lc} = T_f \quad [20]$$

Further, Eq. [4], for the liquid region $0 \le \eta \le 1$, and the boundary conditions at the interface between the solid and liquid and at the position of cast inner surface, $r = r_i$, also can be rewritten as follows, respectively:

$$\frac{\partial T_{lc}}{\partial t} = \frac{\alpha_{lc}}{r_i - s(t)}\left[(1 - \eta)\frac{\partial s(t)}{\partial t} + \frac{1}{r}\right]\frac{\partial T_{lc}}{\partial \eta} + \alpha_{lc}\frac{1}{[r_i - s(t)]^2}\frac{\partial^2 T_{lc}}{\partial \eta^2} \quad (0 \le \eta \le 1) \quad [21]$$

$$\eta = 0,\ T_{lc} = T_{sc} = T_f \quad [22]$$

$$\eta = 1,\ k_{lc}\frac{\partial T_{lc}}{\partial \eta}\frac{\partial \eta}{\partial r} = q_i \quad [23]$$

The heat balance Eq. [15] at the solid-liquid interface for $\xi = 1$ and $\eta = 0$ transforms to

$$\frac{\partial s(t)}{\partial t} = \frac{k_{sc}}{\rho_{sc}H}\left[\frac{1}{s(t)}\frac{\partial T_{sc}}{\partial \xi} - \frac{k_{lc}}{k_{sc}}\frac{1}{r_i - s(t)}\frac{\partial T_{lc}}{\partial \eta}\right] \quad [24]$$

During solidification, the heat generated due to evolution of latent heat depends upon the fraction of solid formed. This heat is assumed to have a linear distribution over the temperature range from T_L to T_S due to an increase in specific heat. Therefore, this is expressed as

$$C_{mc} = C_{lc} + \frac{H}{T_L - T_S} \quad [25]$$

If at time $t = t_n$, $T_{sc} > T_s$ and $t = t_n + \Delta t$, $T_{sc} < T_s$, in the solid region, and at $t = t_n$, $T_{lc} > T_L$ and $t = t_n + \Delta t$, $T_{lc} < T_L$, in the liquid region, the temperature in each region is modified as

$$\text{solid region: } T_{sc}^{t+\Delta t} = T_S - (T_S - T_{sc}^{t+\Delta t})\frac{C_{mc}}{C_{sc}} \quad [26]$$

$$\text{liquid region: } T_{lc}^{t+\Delta t} = T_L - (T_L - T_{lc}^{t+\Delta t})\frac{C_{lc}}{C_{mc}} \quad [27]$$

Since there is no phase transformation, Eqs. [1] and [2] without transformation are used to calculate the steel mold and graphite mold temperature.

B. *Segregation of Particles Due to Centrifugal Forces*

Particle segregation occurs during centrifugal casting because of the difference in density between the molten metal and the particles. A particle which is suspended in molten metal is submitted to a vertical acceleration due to gravity g and to a centrifugal acceleration $\gamma = \omega^2 r$, where r is the distance of the particle to the rotation axis. Generally, γ is much greater than gravity g which allows the vertical movement of the particle to be ignored. Therefore, the different forces on the particle, *i.e.*, the force balance equation on the particle due to centrifugal and viscous forces, can be expressed as follows:[12]

$$\frac{4}{3}\pi R_p^3\,\omega^2 r\,(\rho_p - \rho_l) - 6\pi\eta_{lc}R_p\frac{dr}{dt} = \frac{4}{3}\pi R_p^3\rho_p\frac{d^2r}{dt^2} \quad [28]$$

Equation [28] can be further solved to get the position of the particle at any time t as

$$r(t) = r_0(t)\exp\left[\frac{2\omega^2(\rho_p - \rho_l)R_p^2 t}{9\eta_{lc}}\right] \quad [29]$$

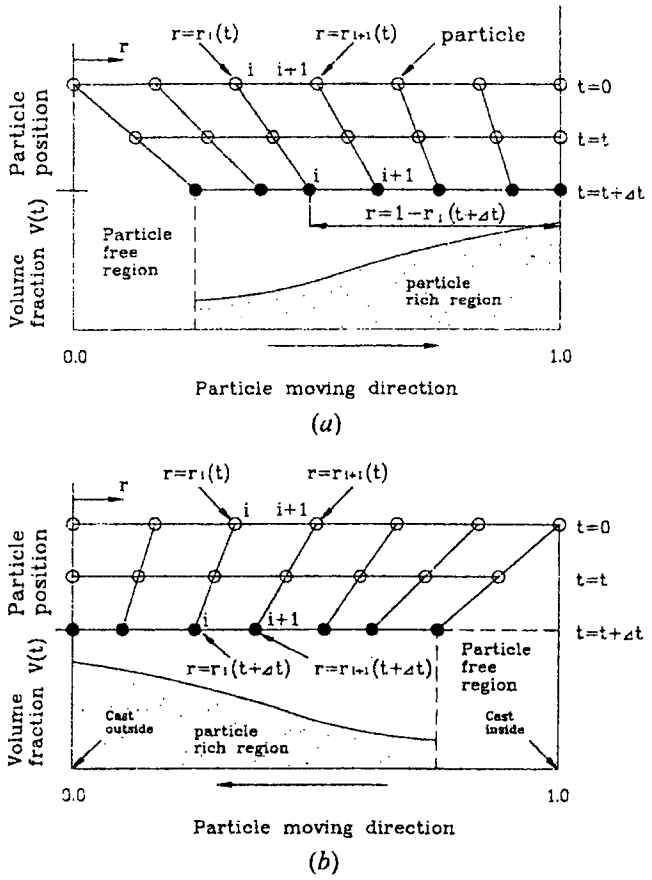

Fig. 3—Particle position and variation of volume fraction due to particle moving: (*a*) $\rho_l > \rho_p$ and (*b*) $\rho_l < \rho_p$.

Table I. Calculation Conditions in Comparison with the Results of the Proposed Model

Physical Properties and Mold Dimension	Lajoye-Suery[19] Model
T_s (°C)	580
T_L (°C)	610
T_m (°C)	150
T_g (°C)	150
T_p (°C)	700
D_s (mm)	180
D_i (mm)	120
R_p (mm)	15.
η (Pa · s)	2.5×10^{-3}

Table II. Physical Properties of the Base Alloy[16]

Physical Properties	Aluminum (A356)	Copper Alloy (C90300)
T_S (°C)	555	854
T_L (°C)	615	1000
T_f (°C)	555	854
H (J/kg)	389	205
C_s, C_l (kJ/kg K)	0.963	0.376
k_s, k_l (W/m K)	159	74
ρ_s, ρ_l (g/cm³)	2.685	8.8
η (mPa • s)	2	4

where $r_0(t)$ is the position of the particle at $t = 0$. To compare a calculated result of the proposed model with Lajoye

Table III. Physical Properties and Size of Reinforcement[17]

Physical Properties	Al_2O_3	SiC_p	Graphite
k (W/m K)	24	25	38
ρ (g/cm³)	4.0	3.2	1.9
C (kJ/kg K)	0.60	0.69	0.71
R_p (μm)	10	10	20

and Suery's model,[19] the centrifugal acceleration $\gamma = \omega^2 r = 100$ g is adopted. The viscosity η_c of the molten metal containing particles is given as follows:[13,14]

$$T > T_L: \eta_c = \eta [1 + 2.5V_f(t) + 10.05 V_f^2(t)] \quad [30]$$

However, in order to estimate the volume fraction due to solidification and particle moving, the viscosity η_c (Eq. [30]) of the particle-rich region containing semisolid materials due to solidification is modified as follows:

$$T < T_L: \eta_c = \eta [1 + 2.5\{V_f(t) + S_f(T)\} + 10.05\{V_f(t) + S_f(T)\}^2] \quad [31]$$

where $S_f(T)$ is the solid fraction due to the solidification of the base alloy and is calculated as follows:[15]

$$S_f(T) = \left[\frac{T_L - T_{lc}}{T_L - T_S}\right]^{1/2} \quad [32]$$

By solving Eq. [29], the thickness of the particle-rich region under various speeds and times has been estimated. Therefore, the variation of a volume fraction at the nodal point i due to particles moving within the liquid region is calculated at time $t = t + \Delta t$ with Eq. [33], as a function of distance from the casting outer surface (Figures 3(a) and (b)). Then, the particle movement is neglected in the mushy state region ($T_S \le T \le T_L$) of the centrifugal casting, because the viscosity sharply increases. The number of particles was taken as the same mesh number ($i = 1$ to 100 in Eq. [33]) of the finite difference method. The volume fraction variation is defined as a function of the moving distance of particles as follows:

$$\rho_l > \rho_p: V_f(t + \Delta t) = V_f(t) \cdot \frac{1 - r_i(t+\Delta t)}{1 - r_i(t)} + V_f(t)\Big|_{t=0}$$
$$\rho_l < \rho_p: V_f(t + \Delta t) = V_f(t) \cdot \frac{r_i(t+\Delta t)}{r_i(t)} + V_f(t)\Big|_{t=0} \quad [33]$$

III. RESULTS AND DISCUSSION

An explicit type finite difference method scheme was used to solve Eqs. [1] through [4] and [18] through [23] with boundary conditions, Eq. [24], at the solid-liquid interface.

Thermophysical properties of base alloy reinforcement materials, mold properties and dimensions of the mold, and casting used in the calculations are listed in Tables I through V.

The calculated particle segregations including heat transfer in both phases (solid and liquid regions) are compared with the reported results[19] (Figure 4).

It is shown that the results of particle segregation considering phase transfer and equivalent specific heat during composite centrifugal casting are closed to theoretically cal-

Table IV. Physical Properties of the Steel and Graphite Molds[15]

Physical Properties	Carbon Steel	Graphite Mold
k (W/m K)	57.8	38
ρ (g/cm^3)	7.8	1.9
C (kJ/kg K)	0.481	0.71

Table V. Mold Dimensions to Centrifugal Casting of Metal Matrix Composites and Heat-Transfer Coefficients[5,15]

D_o	215
D_g (mm)	150
D_c (mm)	100
D_i (mm)	80.8
h_1 (W/m^2 K)	10^2, 5×10^2, 10^3, 1.5×10^3
h_2, h_3 (W/m^2 K)	8.4
h_4 (W/m^2 K)	10^4

culated data by Lajoye and Suery.[19] They also show the comparison between theory and experiment in the form of the variation of the particle fraction and report that the difference is not large. In the present work, the heat-transfer coefficients in the centrifugal casting process have been limited. Ebisu[5] used the local heat-transfer coefficient of 8.3 to 7.6 W/m^2 · K at 300 °C mold ambient connecting air during centrifugal casting. In a survey by Ohnaka,[15] the heat-transfer coefficients for moving mold (aluminum continuous casting) are (0.25 to 0.42) $\times$ 10^3 W/m^2 · K in the case of air gap and (1.67 to 2.5) $\times$ 10^3 W/m^2 · K in the absence of air gap. In the case of aluminum mold casting, according to nonexistence or existence of air gap, the heat-transfer coefficient is shown to be from (1.3 to 1.7) $\times$ 10^4 to (1.7 to 2.9) $\times$ 10^3 W/m^2 · K, respectively. Therefore, in this study, the assumed heat-transfer coefficients h_2 and h_3 at the outer surface of the steel mold ($r = r_0$) and casting inner surface ($r = r_i$) are adopted as 8.4 W/m^2 · K, because heat transfer by convection is essentially negligible.

Furthermore, in order to estimate the validity of the heat-transfer coefficient h_1 of the interface between the graphite mold ($r_g = 0.0$) and casting outer surface ($r = 0.0$), the heat-transfer coefficient h_1 in the case of existence or nonexistence of air gap is used in the range from 10^2 W/m^2 · K to 1.5 $\times$ 10^3 W/m^2 · K (Figure 12).

The heat-transfer coefficients between the graphite mold and molten metal have been reported by Kai-ho and Pehlke[18] as 10^2 to 10^5 W/m^2 · K. The heat-transfer coefficient h_4 between the steel and graphite molds used is a constant value of 10^4 W/m^2 · K in the absence of air gap. Since only a few attempts have been made to study the heat-transfer variation, this has made it difficult to design a proper solidification strategy under different operating conditions. More studies on the heat-transfer coefficient of steel, graphite mold, and casting are necessary to understand the physical process better and to provide a database for the design of centrifugal casting processes for composite materials.

The thicknesses of the graphite-rich region and Al_2O_3, SiC_p particle free region at the inner surface of a different time of rotation N = 1750 rpm, as determined by solving Eqs. [29] through [33], are shown in Figures 5 and 6. It is evident from the calculated results that the more solidification time increases, the more the thickness of the particle-rich region decreases, thereby increasing the volume fraction of graphite at the inner periphery and SiC_p, Al_2O_3 particles at the cast outer periphery ($r = 0.0$). The thickness of the graphite-rich region varies from 0.8 to 0.64 cm as the solidification time increases from 4 to 38 seconds, as shown in Figure 5.

In the case with initial volume fraction V_f = 10 pct, the volume fractions of graphite at the inner periphery near the graphite-free region for solidification time variation were determined from Figure 5.

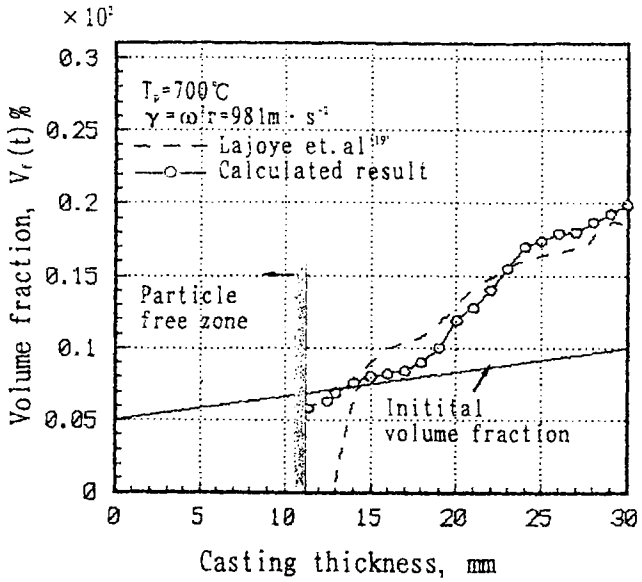

Fig. 4—Comparison between calculated and Lajoye and Suery[19] values for volume fraction variation.

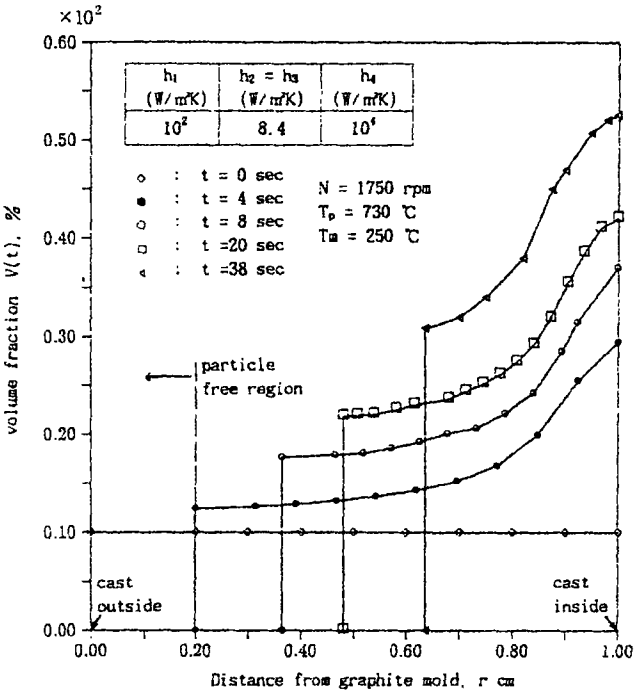

Fig. 5—Effect of centrifugal casting time on graphite particle distribution (initial V_f = 10 pct) in volume fraction of copper alloy containing graphite particles.

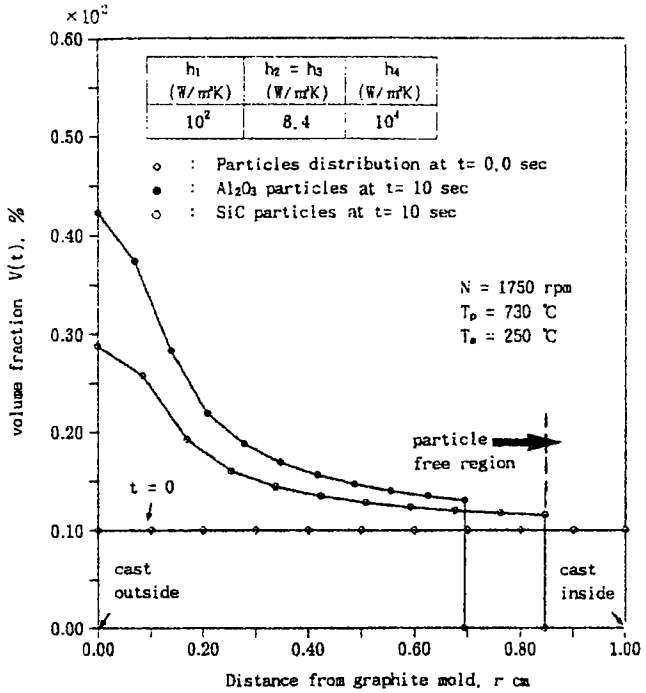

Fig. 6—Comparison of volume fraction variation in centrifugal casting containing Al_2O_3 and SiC_p particles.

A maximum volume percent of about 53 pct graphite was achieved at the inner periphery at solidification time t = 38 seconds. In a similar manner, it was calculated for Al_2O_3 and SiC_p particles with an aluminum base alloy of A356, as shown in Figure 6. In the case of initial volume fraction V_f = 10 pct, the volume fraction variation of the Al_2O_3 particle remarkably increases over that of SiC_p. In the case of initial volume fraction 10 pct Al_2O_3 particles, the volume fraction increases from 10 to 42 pct at the particle-rich region for solidification time t = 10 seconds.

However, the volume fraction variation for SiC_p is less than that of the Al_2O_3 particle reinforced metal matrix composite, as shown in Figure 6. It is observed that the more the density difference between the base alloy and the reinforcement increases, the more the particle segregation increases. The influence of the two kinds of SiC_p and Al_2O_3 reinforced metal matrix composites and A356 base alloy on the movement of the solidification front is illustrated in Figures 7(a) and (b). In the case of the particle-rich region at the inner surface (r = 1.0), such as Al_2O_3, SiC_p reinforced metal matrix composites of Figure 6, the difference in shell thickness between the A356 base alloy and the composite materials at the same solidification time is very large, as shown in Figure 7(a).

However, in the case of the particle-rich region of the casting out surface (r = 0.0), the difference in solidification time to obtain the solidified shell thickness $S(t)$ = 1.0 cm for the copper base alloy and composite materials is very small compared with Figure 7(a). It was observed that the solidification time largely depended on the particle moving direction to effect thermal conductivity of metal matrix composites. Figures 8(a) and (b) show the temperature distribution in the graphite mold ($-2.5 \le r \le 1.0$) and the casting of copper base alloy and copper alloy composites with graphite particles for variations of casting time.

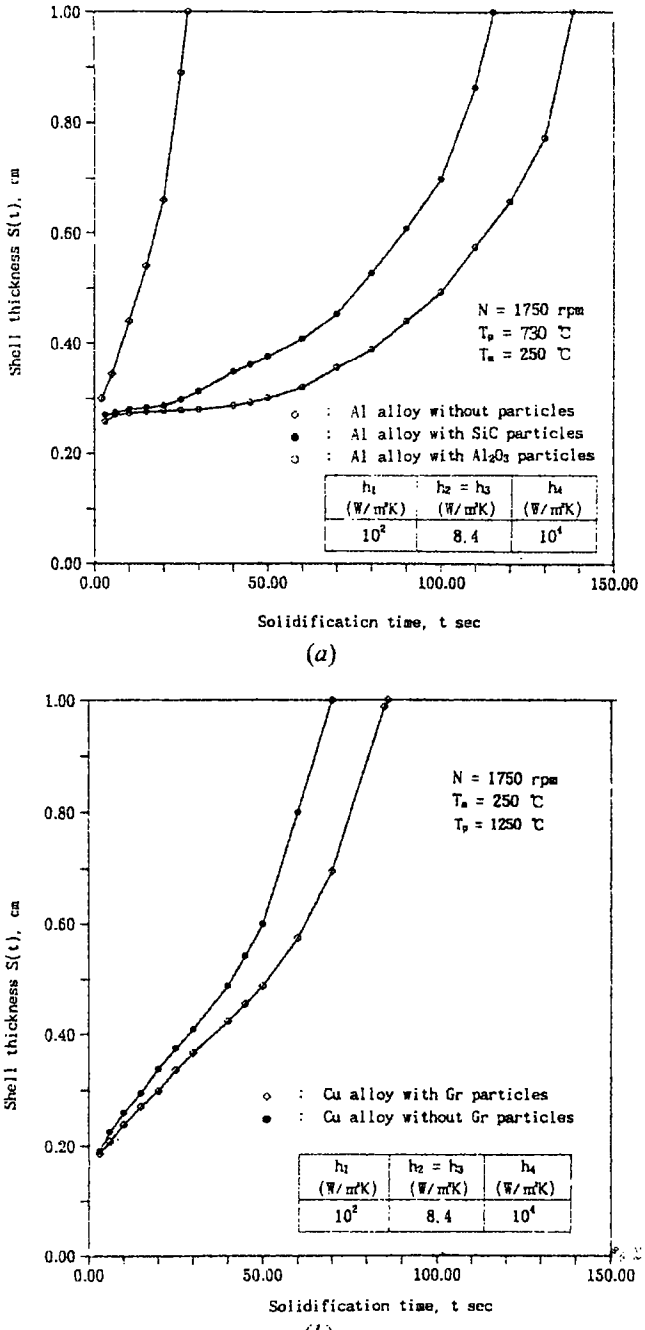

Fig. 7—Effect of reinforcement on solidification time and shell thickness: (*a*) aluminum base alloy and slurry containing SiC_p and Al_2O_3 particles of volume fraction 10 pct; and (*b*) copper alloy and slurry containing a graphite particle of volume fraction 10 pct.

It may be noted that the temperature of the liquid at the inner periphery is 1114 °C, for the base alloy with time t = 10 seconds and, rotational speed N = 1750 rpm. It is the lowest, close to 916 °C, for the base alloy with t = 50 seconds and N = 1750 rpm and about 954 °C at cast inside (r = 1.0) for the composites, as shown in Figure 8(b). These observations clearly indicate that even though in all solidification time ranges the composites containing particles are still in semisolid state (854 °C $\le T \le$ 1000 °C), the copper base alloy solidifies much earlier than the composites.

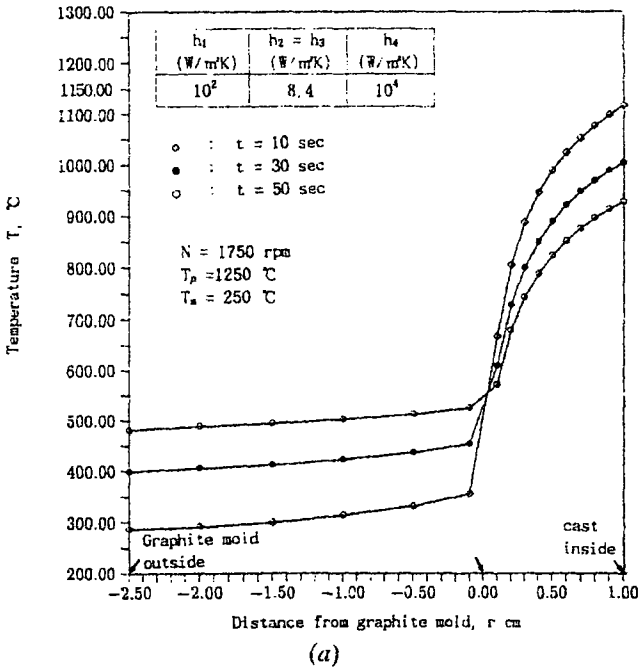

(*a*)

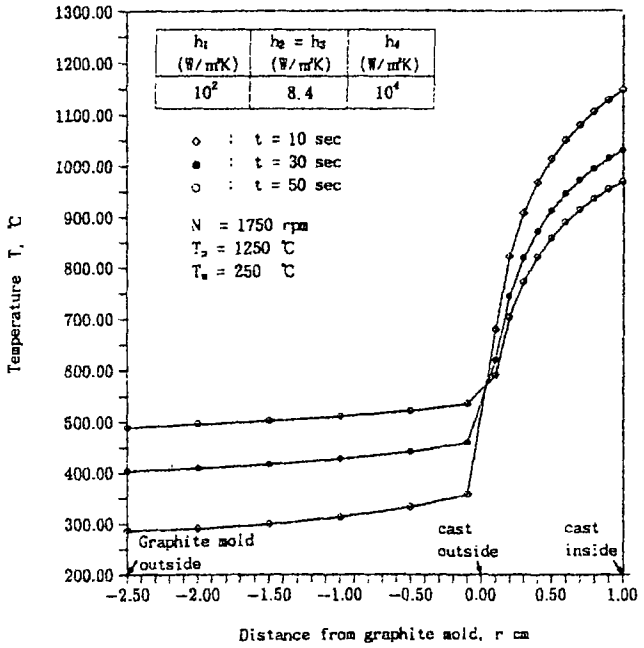

(*b*)

Fig. 8—Effect of solidification time variation on temperature distribution for copper alloy and slurry containing graphite particles: (*a*) copper alloy without particles and (*b*) copper alloy composites with graphite particles of volume fraction 10 pct.

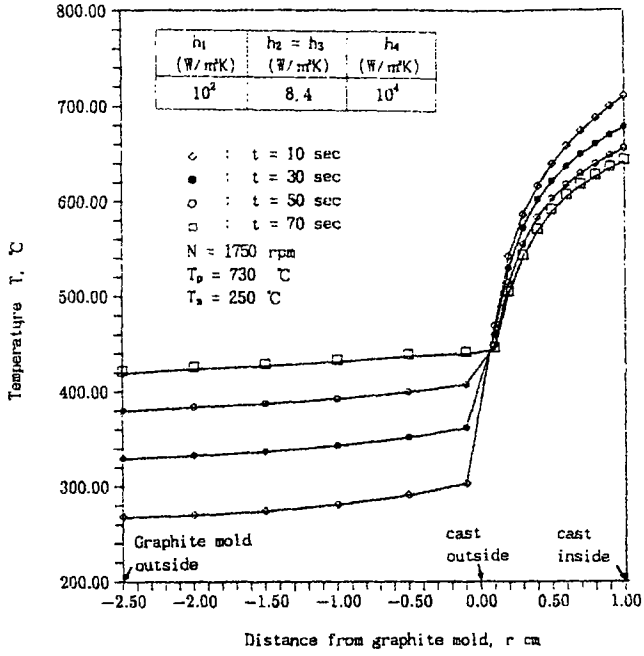

(*a*)

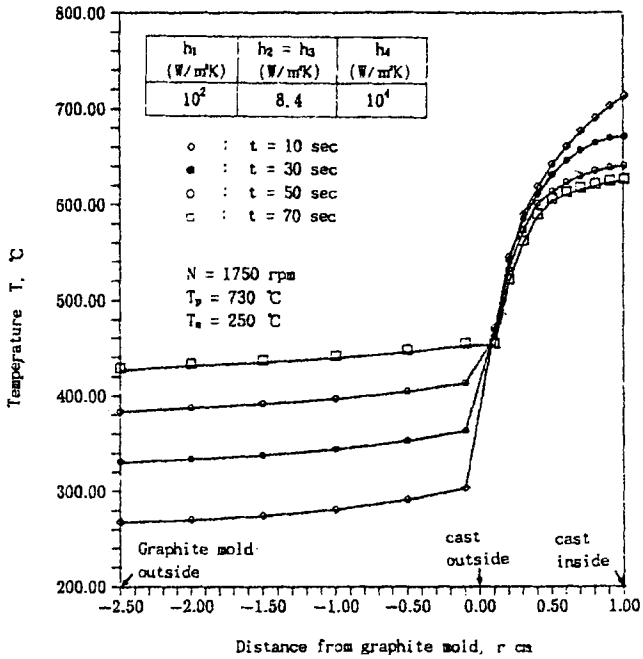

(*b*)

Fig. 9—Effect of solidification time variation on temperature distribution for Al/SiC_p and Al/Al_2O_3 composites with volume fraction 10 pct: (*a*) aluminum silicon particle composites with volume fraction 10 pct and (*b*) aluminum alumina particle composites with volume fraction 10 pct.

Figures 9(a) and (b) show the temperature distribution in the graphite mold ($-2.5 < r < 0.0$) and casting region ($0.0 \le r \le 1.0$) of SiC_p, Al_2O_3 particle reinforced composites for variation of time at $N = 1750$ rpm, $T_p = 730$ °C, and $T_m = 250$ °C. The temperature for the graphite mold and casting regions of the composites is as high as the increasing initial mold temperature $T_m = 250$ °C at a given casting and mold region. Then, the cast region ($0 \le r \le 1.0$) is still in the liquid state above the liquid temperature $T_L = 615$ °C at the lapsed time 70 seconds. Influence of the mold rotation on the movement of the solidification front is illustrated in Figure 10. It is apparent from Figure 10 that the solidification time of the composites containing graphite particles decreases as the rotational speed increases because the heat-transfer coefficient at the casting out periphery ($r = 0.0$), which was in contact with the graphite mold, increases due to particles moving to cast inner periphery ($r = 1.0$).

Figures 11(a) and (b) show solidification time as a func-

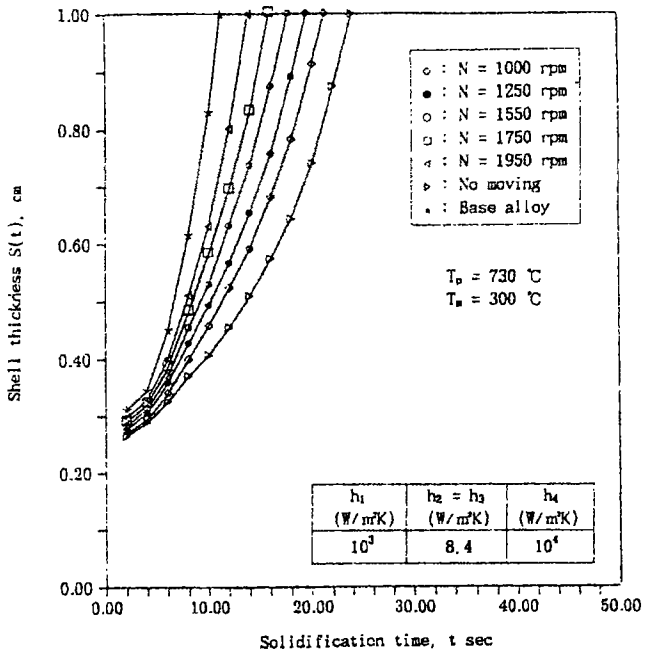

Fig. 10—Effect of rotational speed on solidification time and shell thickness variation on temperature distribution for an aluminum graphite composite with volume fraction 15 pct.

tion of the initial mold temperature T_m for the variation of the heat-transfer coefficient h_1 between the graphite mold inside ($r_g = 0$) and casting outside ($r = 0$). The solidification time increases with an increase in T_m, as shown in Figures 11(a) and (b).

Figures 11(a) and (b) show, as expected, that a higher heat-transfer coefficient resulted in more rapidly solidified composite materials. Figure 12 shows the temperature distribution for various parameter values of the heat-transfer coefficient h_1. It is seen that the higher the value of h_1, the lower the temperature distribution between the graphite mold ($-2.5 \le r \le 0.0$) and the casting region ($0.0 \le r \le 1.0$).

During solidification of the binary and multicomponent alloys, the solidification front is not always smooth, and under most practical conditions, a variety of microscopically complicated growth structures is developed. The present study is largely based on a simplified equivalent specific heat for the phase-change process during the centrifugal casting process. The temperature variation due to the specific heat change in a mushy region was modified by Eqs. [26] and [27].

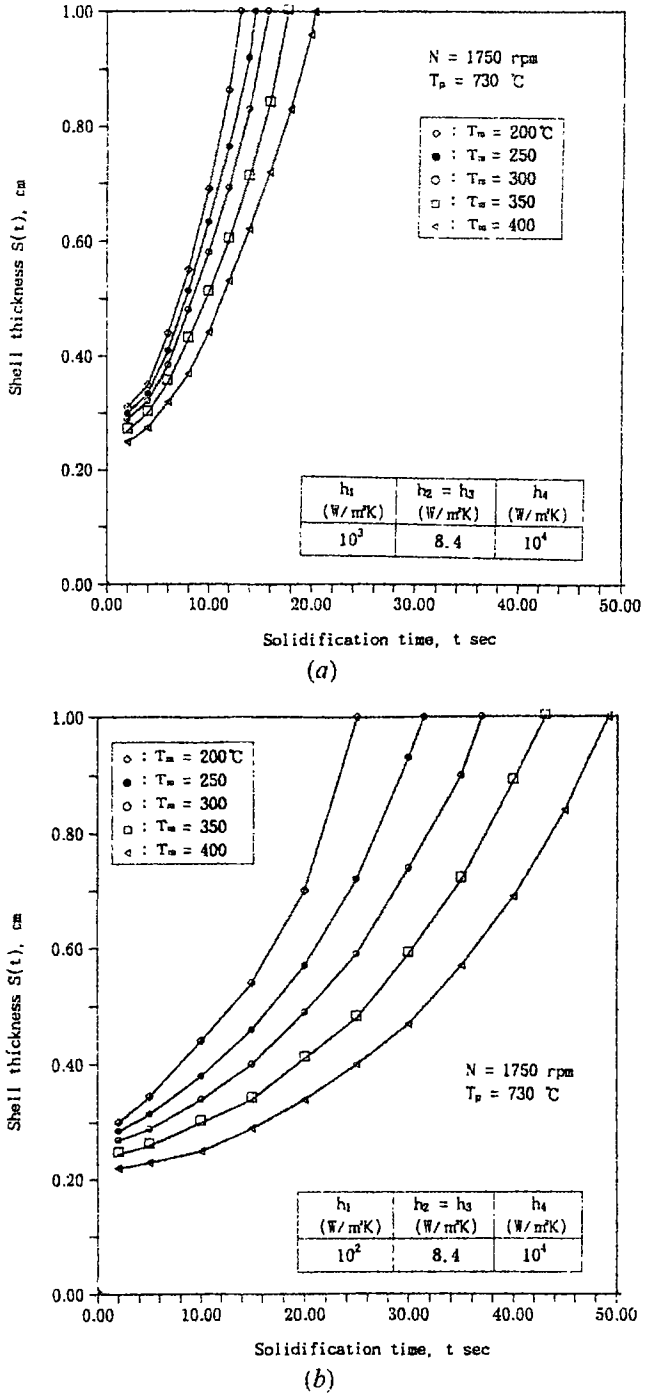

Fig. 11—Effect of initial mold temperature on solidification time and shell thickness with aluminum graphite composite of volume fraction 15 pct for various heat transfer coefficients between graphite mold and cast outside: (*a*) $h_1 = 10^3$ W/m² K and (*b*) $h_1 = 10^2$ W/m² K.

IV. CONCLUSIONS

The heat-transfer analysis during the centrifugal casting of Al_2O_3/Al, SiC_p/Al, Cu/Gr, and composite materials indicates the following.

1. The numerical modeling of particle segregation during centrifugal casting of liquid metal containing suspended particles was proposed.
2. The volume fraction of graphite at the inner periphery of the cylinder and near the graphite-free region is a strong function of mold rotational time. A maximum of 52 vol pct graphite can be concentrated at the inner periphery at a solidification time of 38 seconds. A minimum of 12 pct volume fraction graphite can be concentrated near the graphite-free region at time $t = 4$ seconds and mold rotation speed $N = 1750$ rpm.
3. The temperature of the liquid region at the inner periphery of the composite cylinder depends on the speed of rotation, variation of reinforcement, and base alloy. For instance, with no mold rotation, the solidification time to get casting thickness 1.0 cm was estimated to be 23.8

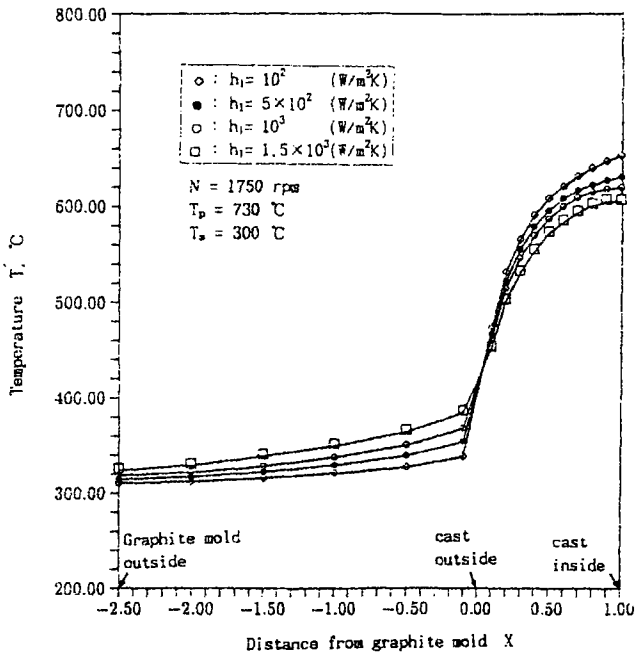

Fig. 12—Effect of heat transfer coefficient on temperature with aluminum graphite composites of volume fraction 15 pct and lapsed time 10 s.

seconds for the aluminum graphite composites and 11.3 seconds for the aluminum base alloy without graphite.

4. The initial temperature of the mold and the speed of mold rotation significantly influence the solidification time due to the particle segregation as a function of volume fraction.

NOMENCLATURE

C	specific heat
h_1, h_2, h_3, h_4	heat-transfer coefficient of $r = 0$, $r = r_i$, $r = -r_0$, and $r = -r_g$, respectively
H	latent heat of solidification
i	number of particles to volume fraction calculation
k	thermal conductivity
N	mold rotational speed
R_p	particle radius
r	coordinate system
r_i	composite cylinder (casting inner) thickness
r_g	distance from casting inside to graphite mold outside
$r_0(t)$	position of particle at $t = 0$
$r_i(t + \Delta t)$	position of ith particle at time $t + \Delta t$
$r_i(t)$	position of ith particle at the time t
$s(t)$	solidification front as a function of time
T	temperature
T_g	temperature of graphite mold
T_L	liquidus temperature of base alloy
T_{lc}	temperature of liquid region for composites
T_S	solidus temperature of base alloy
T_{sc}	temperature of solid region for composites
T_f	solidification front temperature
T_p	pouring temperature
T_m	temperature of steel mold
t	time
Δt	time increment
$V_{p(i)}\|t = 0$	volume fraction at time $t = 0$ (initial volume fraction)
$V_p(t + \Delta t)$	volume fraction of particle as function of time $(t + \Delta t)$
ρ_p, ρ_l	Density of particle and base alloy, respectively
α	thermal diffusivity
η	viscosity of base alloy
ω	angular velocity of mold
δ_1	air gap between cast and graphite mold
δ_2	air gap between graphite mold and steel mold

Subscripts

g	graphite mold
gi	position of graphite mold inside for $r = -\delta_1$
go	position of graphite mold outside for $r = -r_g$
L	liquid region of base metal
lc	liquid region of composite materials m: steel mold
mc	mushy region of composite materials
mi	position of steel mold inside for $r = -(\delta_2 + r_g)$
n	time-step
oa	position of steel mold ambient $r = -r_0$
oc	position of casting outer surface at $r = 0$
oi	position of cast inner surface ambient
p	particle
ri	position of cast inner surface $r = r_i$
S	solid region of base metal
sc	solid region of composite materials

REFERENCES

1. M. Suery and L. Lajoye: *Solidification of Metal Matrix Composites*, Proc. Conf., P.K. Rohatgi, ed., TMS, Warrendale, PA, 1990, pp. 171-79.
2. C. Vaidyanathan, R. Rohrmayer, and C.R. Loper: *8th. Int. Conf. Compos. Mater.*, 1991, p. 17-0-1.
3. M.N. Gungor: *8th Int. Conf. Compos. Mater.*, 1991, p. 18-G-0.
4. B.P. Krishnam, H.R. Shetty, and P.K. Rohatgi: *AFS Trans.* 1976, vol. 76, pp. 73-80.
5. Y. Ebisu: *AFS Trans.*, 1977, vol. 77, pp. 643-54.
6. O.H. Wustrack: *AFS Cast Mold Res. J.*, 1973, Mar. p. 11.
7. A. Lazaridis: *AFS Cast Met. Res. J.*, 1970, Dec., 153.
8. A. Khan: Ph.D. Dissertation, The University of Wisconsin–Milwaukee, Milwaukee, 1990.
9. W. Kurz and D.J. Fisher: *Fundamentals of Solidification*, Trans Tech Publications, 1989, pp. 63-74.
10. T. Saitoh: *Trans. ASME*, 1978, vol. 100, p. 294.
11. T. Saitoh, H. Hojo, H. Yaguchi, and C.G. Kang: *Metall. Trans. B*, 1989, vol. 20B, pp. 381-90.
12. J. Szekely: *Fluid Flow Phenomena in Metals Processing*, Academic Press, New York, NY, 1979, pp. 255-63.
13. D.M. Stefanescu, A. Moitra, A.S. Kacar, and B.K. Dhindaw: *Metall. Trans. A*, 1990, vol. 21A, pp. 231-39.
14. D.M. Stefanescu and B.K. Dhindaw: *Metals Handbook*, ASM INTERNATIONAL, Metals Park, OH, 1988, vol. 15, pp. 142-47.
15. I. Ohnaka: *Introduction to Heat and Solidification Analysis by Computer* Maruzen Press, 1985, pp. 326-40 (in Japanese).
16. *Metals Handbook*, 10th ed., ASM INTERNATIONAL, Materials Park, OH, 1990, vol. 2, pp. 164 and 374.
17. M. Taya and R. Arsenault: *Metal Matrix Composites*, Pergamon Press, Elmsford, NY, 1989, pp. 244-49.
18. Kai-Ho and R.D. Pehlke: *Metall. Trans.*, B1985, vol. 16B, pp. 585-94.
19. L. Lajoye and M. Suery: in *Cast Reinforced Metal Composites*, S.G. Fishman and A.K. Dhingra, eds. ASM INTERNATIONAL, Metals Park, OH, 1988, pp. 15-20.